Wavelength tuning of an antenna-coupled infrared microbolometer

Michael A. Gritz[a)]
Raytheon, Space and Airborne Systems, Electronic Warfare Systems, 6380 Hollister Avenue, Goleta, California 93117

Meredith Metzler
Cornell NanoScale Facility, Cornell University, Ithaca, New York 14853-5403

Donald Malocha
Department of Electrical and Computer Engineering, University of Central Florida, Orlando, Florida 32816-2362

Mohamed Abdel-Rahman, Brian Monacelli, Guy Zummo, and Glenn D. Boreman
CREOL/School of Optics, University of Central Florida, Orlando, Florida 32816-2700

(Received 2 June 2004; accepted 13 September 2004; published 10 December 2004)

Wavelength tuning is demonstrated in an antenna-coupled infrared microbolometer. With a 300-mV control voltage, we observed a tuning range of 0.15 μm near 10 μm. A metal-oxide-semiconductor capacitor underneath the antenna arms causes the shift of resonance wavelength with applied voltage. We develop a device model that agrees with measured results. © *2004 American Vacuum Society.* [DOI: 10.1116/1.1813465]

I. INTRODUCTION

Conventional bolometers have long been used as thermal detectors for infrared (IR) radiation, using the change of resistance with an increase in the temperature. In the case of antenna-coupled microbolometers,[1,2] incident radiation induces IR-frequency current waves in the arms of the antenna, which are dissipated in the subwavelength-sized bolometer. One of the main advantages of antenna coupling of IR sensors is that their polarization[3] and wavelength responses can be electrically tuned by control of the current waves propagating on the antenna arms. In this article, we present the first demonstration of wavelength tuning in an antenna-coupled infrared microbolometer. The tuning mechanism is derived from a metal-oxide-semiconductor (MOS) capacitor underneath the arms of the antenna. Controlling the capacitance of this MOS capacitor by a small dc voltage modifies the electrical length of the antenna, thus tuning the free-space resonant wavelength.

II. DEVICE MODEL

A cross section of the device along with its equivalent circuit is shown in Fig. 1, with full length of the antenna $b=1.7\ \mu\text{m}$, cross arm width $a=0.385\ \mu\text{m}$, distance from contact to feed point $d=0.95\ \mu\text{m}$. The thickness h of the sputtered SiO_2 insulator layer is 25 nm, and the substrate is 8000 Ohm-cm p-type Si with $N_A=4\times10^{11}\ \text{cm}^{-3}$.

A transmission-line model was developed for the antenna and MOS-capacitor combination. The MOS capacitor acts as a varactor (C_{mos}), in series with the antenna capacitance C_a. Their equivalent capacitance C_{eq}, is in parallel with the antenna inductance L_a and the fringe-field capacitance C_f. The resonance frequency (f_r) for the antenna is given by

$$f_r=\frac{1}{2\pi\sqrt{L_t(C_{\text{eq}}+C_f)}}. \quad (1)$$

We model C_{eq} as a function of voltage using an exact-charge distribution model[4]

$$C_{\text{eq}}=\frac{C_a}{1+\left(\frac{\varepsilon_{\text{SiO}_2}W_{\text{eff}}}{\varepsilon_{\text{Si}}h}\right)}, \quad (2)$$

where W_{eff} is the effective width of the depletion region, given by

$$W_{\text{eff}}=\begin{cases} U_SL_D\left[\dfrac{2F(U_S,U_F)}{e^{U_F}(1-e^{-U_S})+e^{-U_F}(e^{U_S}-1)}\right] & \text{accumulation region} \\ \dfrac{\sqrt{2}L_D}{(e^{U_F}+e^{-U_F})^{1/2}} & \text{flat band} \\ U_SL_D\left[\dfrac{2F(U_S,U_F)}{e^{U_F}(1-e^{-U_S})+e^{-U_F}(e^{U_S}-1)}\right] & \text{depletion region/inversion} \end{cases}, \quad (3)$$

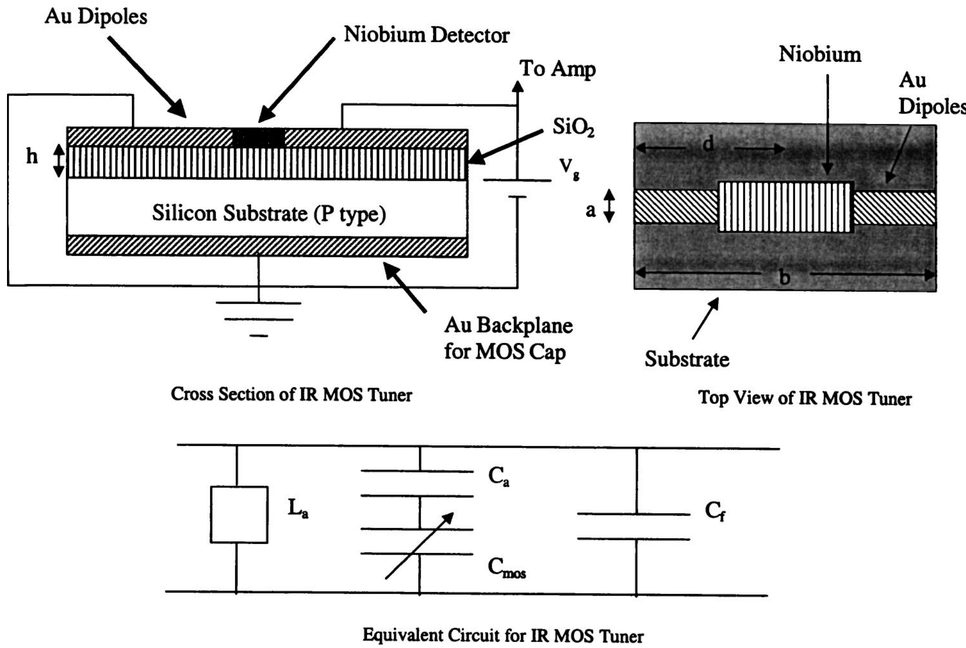

FIG. 1. (a) Cross section of IR MOS Tuner. (b) Top view of IR MOS Tuner. (c) Equivalent circuit for IR MOS Tuner.

where L_D is the intrinsic Debye length,

$$L_D = \sqrt{\frac{\varepsilon_{\mathrm{Si}}\varepsilon_o kT}{2q^2 n_i}} \tag{4}$$

in which $n_i = 1\times 10^{10}\ \mathrm{cm}^{-3}$ is the intrinsic concentration of Si. We use the intrinsic and Fermi energies in the Si to find the surface potential

$$U_S = \frac{E_i(\mathrm{bulk}) - E_i(\mathrm{surface})}{kT} \tag{5}$$

and the doping parameter

$$U_F = \frac{E_i(\mathrm{bulk}) - E_F}{kT}. \tag{6}$$

With the definition of the function

$$F(U_S, U_F) = \sqrt{e^{U_F}(e^{-U_S} + U_S - 1) + e^{U_F}(e^{U_S} - U_S - 1)}. \tag{7}$$

Since we are using an exact charge distribution model, the capacitance cannot be expressed as a function of the applied voltage. However both variables are related to U_S, therefore the capacitance expected for a given applied voltage including the metal-semiconductor work function difference can be found using[4]

$$V_G = \frac{kT}{q}\left[U_S + \hat{U}_S \frac{\varepsilon_{\mathrm{Si}} h}{\varepsilon_{\mathrm{SiO_2}} L_D} F(U_S, U_F) + \phi_{\mathrm{Au}} - \ln\left(\frac{N_A}{n_i}\right) - \frac{E_g}{2}\right], \tag{8}$$

where $\hat{U}_S = 1$ if $U_S > 0$ and -1 if $U_S < 0$, and $\phi_{\mathrm{Au}} = 0.7$ eV is the work function for Gold, and $E_g = 1.1$ eV) is the band-gap energy of Si.

[a)]Author to whom correspondence should be addressed; electronic mail: Michael_A_Gritz@raytheon.com

Equation (2) for C_{eq} can then be evaluated, knowing C_a of the microstrip dipole antenna, which can be found using[5]

$$C_a = \frac{\varepsilon_0 \varepsilon_r ab}{2h} \cos^{-2}\left(\frac{\pi d}{b}\right), \tag{9}$$

where the average relative permittivity (ε_r) of the substrate is calculated as

$$\varepsilon_r = \frac{\varepsilon_{\mathrm{SiO_2}}\varepsilon_{\mathrm{Si}}}{\varepsilon_{\mathrm{SiO_2}} + \varepsilon_{\mathrm{Si}}}. \tag{10}$$

The inductance L_a of the antenna can be calculated from Eq. (1) as

$$L_t = \frac{1}{\omega^2 C_{\mathrm{eq}}}. \tag{11}$$

For calculation of the fringe-field capacitance C_f, we consider that the microstrip has electrical dimensions greater than its physical dimensions. For the antenna shown in Fig. 1, the fringing affects the cross-arm width a of the dipole. The difference is found as[6]

$$\Delta a = 0.412\, h \frac{(\varepsilon_r + 0.3)\left(\frac{a}{h} + 0.264\right)}{(\varepsilon_r - 0.258)\left(\frac{a}{h} + 0.8\right)}. \tag{12}$$

Now C_f can be found, where $\lambda_r = 10.45\ \mu$m is the initial measured resonant wavelength, using[5]

$$C_f = \frac{0.016\,68\ \varepsilon_r}{\omega}\left(\frac{\Delta a}{h}\right)\left(\frac{a}{\lambda_r}\right). \tag{13}$$

Using Eq. (1), with results from Eqs. (2), (11), and (13), allows us to find the free-space resonant wavelength ($\lambda = c/f$) of the IR MOS tuner as function of applied voltage V_G. The results of this model are shown in Fig. 2, along with

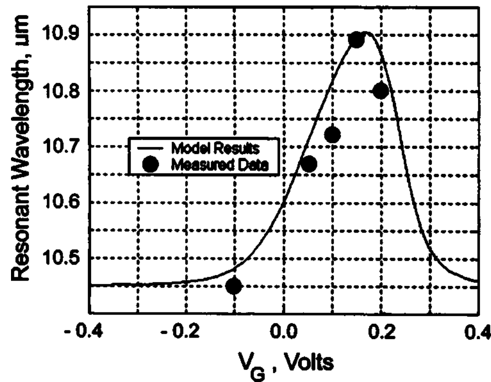

FIG. 2. Comparison of model and measured data for the wavelength-tuned antenna.

measured values. When the device was biased beyond 150 mV, the resonance of the device begins to shift towards shorter wavelengths.

III. FABRICATION AND RESULTS

The IR MOS tuners were fabricated at the Cornell NanoScale Facility using a Cambridge/Leica EBMF 10.5 e-beam lithography system. Figure 3 shows a block diagram of the fabrication used. Both local and global alignment marks were then written using a bilayer of poly(methylmethacrylate and methacrylic acid) (PMMA-MAA) and poly(methylmethacrylate) (PMMA) in a liftoff process. The global marks were used to correct for any rotation errors while loading the substrates into the chuck, while the local marks were used to correct for any stage drift when moving from field to field. Gold was used for the dipole antenna arms with niobium as the bolometer.

We fabricated the MOS capacitor with 25 nm of sputtered SiO_2 on top of a p-type Si substrate, with a dipole antenna with a full antenna length of 1.7 µm. The dipole antenna-coupled microbolometer was fabricated on top of a three-inch Si wafer with a resistivity of 8000 Ω cm ($N_A=4\times10^{11}$ cm^{-3}). The width of the antenna arms fabricated was 385 nm. A scanning election microscopy (SEM) micrograph of one of the devices fabricated is shown in Fig. 3.

We used a tunable CO_2 laser with emission from 9.28 to 10.78 µm in discrete lines. The laser was focused by a F/1 optical train. The laser polarization was linear and was rotated by means of a half wave plate. The bolometer under test was placed at the focus of the beam. The position of the device was adjusted for the best response by using motorized stages with submicron accuracy. The beam was modulated with a chopper at a frequency of 2.5 kHz. The modulated signal was read with a lock in amplifier after a 10 $\times$ preamplification. For the device under test, the maximum signal V_{max} was obtained for the polarization parallel to the antenna axis and the minimum signal V_{min} for the cross polarization. The polarization dependent signal is defined as $\Delta V = V_{max} - V_{min}$. The polarization dependant signal and the power on the detector were measured for each wavelength. The power fluctuation from the laser output for each wavelength was removed from the measured signal by normalization of the polarization signal [volts] to the measured power [watts] on the detector.

The bolometer under test was biased with both positive (depletion mode) and negative voltages (accumulation mode)

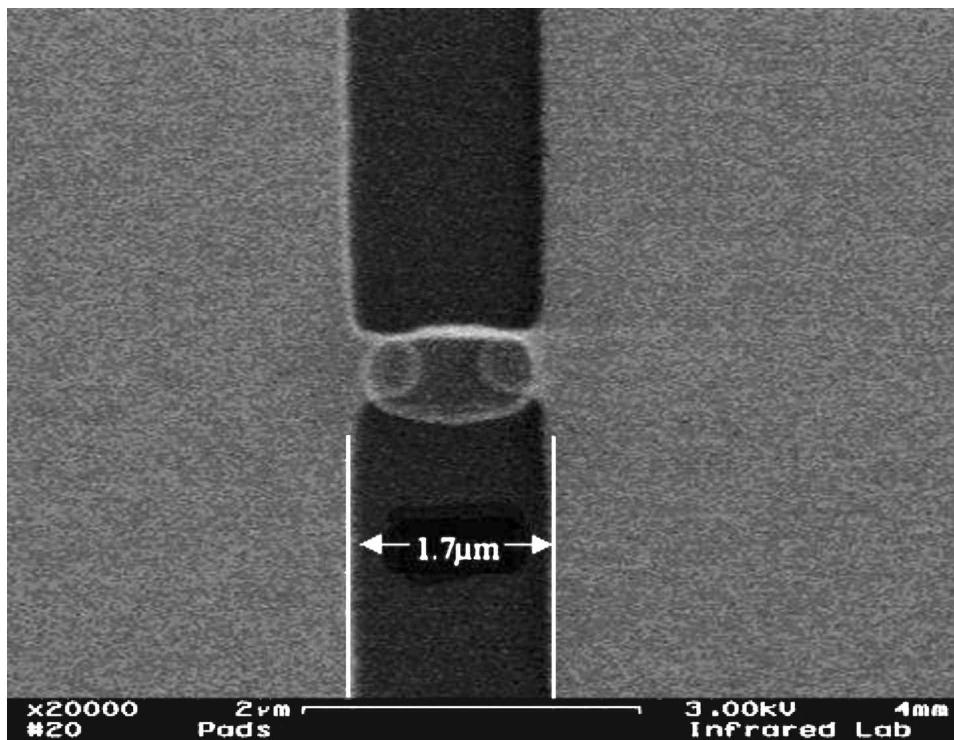

FIG. 3. SEM micrograph of 1.7 µm dipole antenna-coupled microbolometer IR MOS tuner.

and placed at the focus of the beam. The device was first measured with a bias of −100 mV. Then the device bias was changed to a positive bias, which was adjusted in 50 mV increments up to 200 mV. The discrete-line results of each measurement were then fitted to a Gaussian profile using a least-squares fit in order to find the precise resonance of the dipole antenna at each biasing voltage. These data for resonance wavelength as a function of bias voltage are seen in Fig. 2.

IV. CONCLUSIONS

An antenna-coupled IR bolometer was demonstrated to have tunable wavelength reponse near 10 μm, with around 0.5 μm of tuning. The tuning mechanism is MOS capacitor developed underneath the antenna structure in a Si substrate. A model was developed for the tuning behavior that agrees well with measured values. Trends in this model indicate that the tuning range is increased for thinner oxide layers and for lower doping concentrations. Our device was thus fabricated with an oxide layer of 25 nm and a substrate resistivity of 8000 Ω cm.

ACKNOWLEDGMENTS

This work was performed in part at the Cornell Nanofabrication facility (a member of the National Nanofabrication Users Network), which is supported by the National Science Foundation under Grant No. ECS—9731293, Cornell University, and industrial affiliates. This material is based upon research supported by NASA Grant No. NAG5—10308.

[1]E. Grossman, J. Sauvageau, and D. McDonald, Appl. Phys. Lett. **59**, 3225 (1991).
[2]I. Codreanu, C. Fumeaux, D. Spencer, and G. Boreman, Electron. Lett. **35**, 2166 (1999).
[3]G. Boreman, C. Fumeaux, W. Herrmann, F. Kneubühl, and H. Rothuizen, Opt. Lett. **23**, 1912 (1998).
[4]R. F. Pierret, *Semiconductor Device Fundamentals*, Chap. 16 (Addison-Wesley, New York, 1996).
[5]S. K. Sharma and B. R. Vishvakarma, Int. J. Electron. **86**, 979 (1999).
[6]C. Balanis, *Antenna Theory Analysis and Design*, Chap. 4 (Wiley, New York, 1997).